

Article

Structural Performance of uPVC Confined Concrete Equivalent Cylinders Under Axial Compression Loads

Abraham Mengesha Woldemariam ^{1,*} , Walter O. Oyawa ² and Timothy Nyomboi ³

¹ Civil Engineering Department, Pan African University Institute for Basic Sciences, Technology and Innovation (PAUSTI), 62000 JKUAT, Nairobi 00200, Kenya

² Civil, Const. and Environmental Engineering Department, Jomo Kenyatta University of Agriculture and Technology (JKUAT), PAUSTI and CUE, 62000 JKUAT, Nairobi 00200, Kenya; oyawaw@yahoo.com

³ Department of Civil and Structural Engineering, PAUIST and Kenya Urban Roads Authority, 62000 JKUAT, Nairobi 00200, Kenya; tnyomboi@hotmail.com

* Correspondence: abrish27@yahoo.com

Received: 11 March 2019; Accepted: 3 April 2019; Published: 14 April 2019



Abstract: There is always a need for more durable, ductile, and robust materials for buildings, bridges, and other infrastructure due to the drawbacks of existing construction materials. Some of the drawbacks are the corrosion of steel, the brittle failure of concrete, and the performance instabilities that are caused when exposed to different environments. Thus, an innovative system is required to improve the performance and retain the integrity of structures in a harsh environment. To alleviate the situation, Un-plasticized polyvinyl chloride (uPVC) tubes are used as a confining material and their performance was experimentally evaluated by testing uPVC confined equivalent cylinders. Accordingly, unconfined and uPVC confined equivalent concrete cylinders for five different concrete classes, four types of uPVC tube sizes, and the aspect ratios of two ($h/D = 2$) were prepared and tested under axial compression loads. The result shows that the uPVC confinement increased the strength, ductility factor, and energy absorption in between 1.28–2.35, 1.84–15.3, and 11–243 times the unconfined levels, respectively. The confinement performed well for lower concrete classes and higher thickness to diameter ratios ($2t/D$). The post-peak behavior of the stress-strain curve was affected by the $2t/D$ ratio and the absolute value of the slope decreased as the $2t/D$ ratio increased. Additionally, the uPVC tube has shown several advantages, such as acting as a permanent formwork, protecting the concrete from chemical attacks, preventing the segregation of concrete, preventing peeling, and taking off concrete cover, decreasing the cross-section, and resulting in lighter sections. The uPVC confinement provided a remarkable improvement on the strength, ductility, energy absorption, and post-peak behavior of concrete. Therefore, uPVC tubes can be used as confining material for bridge piers, piles, electric poles, and highway signboards, where the fire risk is very small, though additional research is required on fire resistance mechanisms, such as wire-mesh reinforced mortar cover.

Keywords: confinement; ductility; energy absorption; strength; stress-strain; uPVC-confined concrete

1. Introduction

The peeling of concrete covers, permeability and steel corrosion of reinforced concrete structures are some of the challenges that engineers face from time to time. The extent of damage of reinforced concrete (RC) structures depend on the environment that they are exposed to and the exposure conditions are dynamic, which makes it difficult to quantify/predict the effect on RC structures. In the last few decades, a substantial number of research studies have been focused on finding an alternative

material to replace steel reinforcements and increase the ductility of concrete. Recent development regarding the use of fiber reinforced polymer (FRP) as a reinforcement and confinement on concrete structures has shown a positive result. The use of FRP in FRP confined concrete increased the strength and reduced the peeling of concrete cover, permeability, and alkali attacks. However, the lack of material ductility delayed the use of FRP as reinforcement. In the recent past, the ductile failure of plastics (polyvinyl chloride) gained the attention of researchers to use it as a confining material in concrete. Plastics (Un-plasticized polyvinyl chloride (uPVC) tubes) have the potential to increase the strength, ductility, energy absorption and durability. However, knowledge on the use of plastic tubes in construction is scattered and lacks information regarding how to design a concrete confined in a plastic tube [1,2].

Un-plasticized polyvinyl chloride (uPVC) is a family of polymers that is made from a chain of a long hydrocarbon and it is the most commonly used polymer families for plumbing purposes. When compared to polyvinyl chloride (PVC), uPVC is strong, stiff, hard, and does not burn by itself [2–8]. uPVC is resistant to corrosion, abrasion, acids, salts, and bases, which provides the advantage of its use as a structural material in any such environment [1,2]. Additionally, polyethylene copolymer coatings have been used to protect the external surface of onshore and offshore pipelines for more than a century [7]. The durability of uPVC was investigated by dipping the uPVC specimen in acid, alkaline, and organic compounds for a time. The predicted service life shows that uPVC has the potential of retaining its integrity without deterioration for more than 50 years [1,2,8–10]. Experimental investigations regarding damage initiation, stress deterioration, crack initiation and growth, impact tests, bursts, and the tensile and fatigue of PVC have exhibited remarkable performance, in that its service life may extend beyond 100 years [2,11–14]. In addition, plastic (uPVC) has a lower thermal conductivity of about 0.45% of a steel tube, which makes it a suitable environment to cure core concrete when compared to a steel tube [15,16].

Previous research has shown the improved strength and ductility of concrete when laterally confined by uPVC pipes. However, the use of uPVC pipes as a concrete confining material is at its very beginning and the amount of information on how to design and use it in construction is very limited. It has been established that providing a uPVC lateral confinement can enhance the strength and ductility of concrete [4–6,9,17–19]. Gupta and Verma [8] investigated the durability through submerging the PVC confined RC column for six months into a salt concentration, which is more than 20 times more so than natural seawater. The finding shows that confining the RC columns using a PVC tube that was protected the column from the aggressive environment and contributed to the long-term durability of the structure. Marzouk and Sennah [20] did some work on PVC confined short columns under axial compression and the ultimate compressive strength increased between 11–17% of the unconfined strength. Wang and Yang [15] carried out an experiment on PVC confined columns having a PVC tube diameter of $D = 100$ mm, concrete grade of C30, C45, and C60, and height to diameter ratio of $h/D = 2$ under concentric loading. The compressive strength and strain increased in between 1.324 to 2.345 and 2.094 to 5.540 times when compared to the unconfined column, respectively.

Oyawa et al. [5] reported a similar finding on the strength of axially loaded uPVC confined stub columns with different uPVC tube diameters, concrete grades, and height to diameter ratios. The confined compressive strength increment ranged from in between 1.18 to 3.65 times the unconfined strength. Additionally, Saadoon [21] investigated PVC encased concrete columns. The proposed system increased the strength and strain up to 168.8 and 147.3%, respectively. Similarly, Jamaluddin et al. [19] used PVC tubes to encase the concrete columns to study the performance of PVC tube confined columns. The proposed system increased the strength and strain up to 40%. In a similar study, which confirmed that concrete column with PVC tubes increased the strength by 71.8% times when compared to the unconfined column [22]. In addition, Gupta [7] investigated uPVC confined columns having uPVC tube diameters of $D = 140, 160, \text{ and } 200$ mm, concrete grades of C20, C25, and C40, and a height $h = 700$ mm under concentrated load. The compressive strength, ductility, and energy absorption increased by between 1.352 to 2.100, 1.30 to 2.65, and 1.55 to 3.52 times that of the unconfined, respectively.

The literature shows that the use of plastic (uPVC) confinement in uPVC confined concrete improved the structural performance of concrete; however, the findings on strength and ductility are very scattered from one research to another and they are limited in the scope of the study. The effect of uPVC confinement on energy absorption, failure mode, stress-strain (elastic and inelastic), and the post-peak behavior of uPVC confined concrete, as well as how the uPVC confined concrete undergoes straining for the applied load beyond the elastic state has not been fully understood. Therefore, it is necessary to carry out an extensive experimental investigation on the strength, ductility, energy absorption, stress-strain relation, and the mode of failure. The aim of this research is to investigate the performance of concrete-filled uPVC tube equivalent cylinders under pure axial compression. The effect of uPVC confinement on load carrying capacity, strength, ductility, energy absorption, failure mode, stress-strain behavior, and the post-peak stress-strain behavior of uPVC confined concrete are investigated and then compared to the unconfined concrete cylinders.

2. Experimental Program

2.1. Materials

2.1.1. Aggregate

Locally available natural sand from Masinga river (Kenya) and crushed stone that were obtained from Mlolongo (Kenya) were used throughout the experiment. The material characterization was done according to the BS standard and the results are presented in Table 1, Figure 1a,b. The sampling was done according to BS EN 932-1, 1997 [23]. Both the fine and coarse aggregate were graded through sieving and curve plotting according to BS EN 12620: 2013; BS EN 933-1:2012 [24]; and, BS EN 933-2, 1996 [25].

Table 1. Fine and Coarse Aggregate Properties.

Test Type	Specific Gravity	Bulk Density	Water Absorption	Moisture Content	Fineness Modulus
Fine Aggregate	2.62	1479.96 kg/m ³	2.42%	0.28%	3.65
Coarse Aggregate	2.7	1420 kg/m ³	1.34%	1.42%	
Standard	BS EN 1097-6: 2013 [26]	BS EN 1097-6: 2013 [26]	BS EN 1097-6: 2013 [26]	BS EN 1097-5 2008 [27]	BS EN 1097-5 2008 [27]

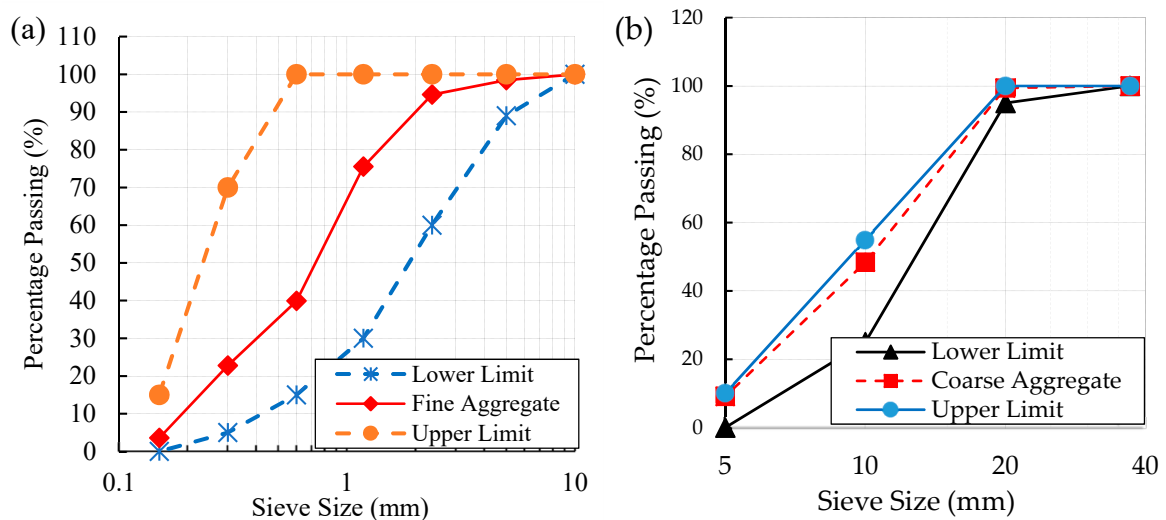


Figure 1. Aggregate grading: (a) fine aggregate, (b) Coarse aggregate.

2.1.2. Cement

The cement that was used in this research was Ordinary Portland cement (OPC) power plus 42.5N manufactured by Bamburi cement Ltd, Kenya. The products conform to European Norm EN 197-1:2011 [28] cement specification and the composition contains 95–100% clinker and 0–5% minor additional constituents by mass.

2.1.3. Concrete Mix Design

Five different types of concrete grades were used. The mix designs were prepared based on BS EN 206: 20134 [29] and BS EN 8500-1/2:2012 [30]. Table 2 summarizes the design values of the constituent material.

Table 2. Concrete mix-design.

Constituent Materials	Cement	Fine Aggregate	Coarse Aggregate	Total Water
Units	kg/m ³	kg/m ³	kg/m ³	kg/m ³
C15	290	667	1253	223
C20	325	632	1253	223
C25	360	602	1247	222
C30	380	582	1247	221
C35	410	552	1247	221

2.1.4. Fresh Properties of Concrete

Conducting tests on a slump, density and compaction factor assessed the fresh properties of concrete. Sampling, slump, density, and compaction factor tests were conducted in accordance with the procedures that are stipulated in BS EN 12350-1: 2009 [31], EN 12350-2: 2009 [32], BS EN 12350-6: 2009 [33], and BS 1881-103: 1993 [34], respectively. Table 3 summarizes the results on the fresh properties of concrete.

Table 3. Fresh properties of concrete mixes.

Fresh Property	Slump	Fresh Density	Compaction Factor
Units	mm	(kg/m ³)	-
C15	60	2418	0.933
C20	60	2431	0.932
C25	60	2433	0.935
C30	60	3438	0.928
C35	60	2451	0.931

2.1.5. Un-Plasticized Polyvinyl Chloride (uPVC) Tube

Un-plasticized polyvinyl chloride (uPVC) pipes that were produced by Elson plastics ltd. (a plastic manufacturing company based in Nairobi, Kenya) were used for this research. The tensile and compressive properties of uPVC are the most important parameters in this study and they are obtained through testing the specimens according to their respective standards.

In multiaxial loading conditions, a material yields when the distortion part exceeds the material yielding stress of the uniaxial tensile test. For a ductile material, von Mises stress (failure criterion) is used to predict the yield stress of material under multiaxial loading, as expressed in Equation (1) where, σ_1 , σ_2 , and σ_3 are the principal stresses and f_y is the yield stress from the tensile test.

$$\sqrt{\frac{1}{2}[(\sigma_1 - \sigma_2)^2 + (\sigma_2 - \sigma_3)^2 + (\sigma_3 - \sigma_1)^2]} \leq f_y \quad (1)$$

The dogbone coupon specimen of uPVC pipe was prepared according to ASTM D638 [35] specification (Figure 2) for the sample that was taken in the direction both parallel and perpendicular to the extrusion in order to check whether there is a variation in the tensile properties along the length and perimeter. The specimens were prepared from two different uPVC pipes having a thickness of 3 and 2.5 mm. The tensile property of uPVC tube was obtained through a tensile test of dogbone coupon specimens, as shown in Figure 2. The test was done by applying a constant rate of 0.083 mm/s according to ASTM D638 [35]; and, an average ultimate tensile strength, Young's modulus of elasticity, and poisson ratio are presented in Table 4 and Figure 3.

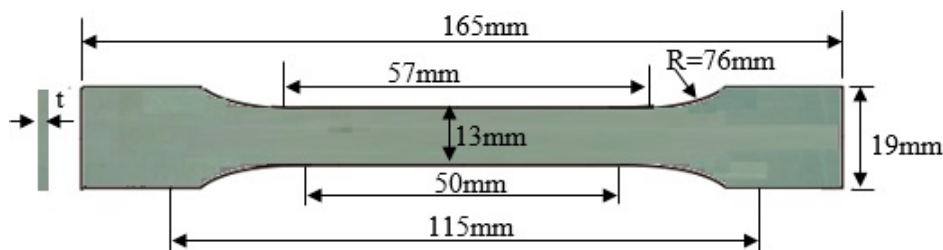


Figure 2. Dog-bone Coupon specimens prepared from the un-plasticized polyvinyl chloride (uPVC) tube (based on ASTM D638).

Table 4. Average values from the tensile strength test.

Parameter	Ultimate Tensile Strength (MPa)	Young's Modulus (GPa)	Poisson Ratio
Parallel to the Extrusion	49.74	3.58	0.342
Perpendicular to the Extrusion	50.10	3.61	0.339
Variance (%)	0.72	0.84	0.880

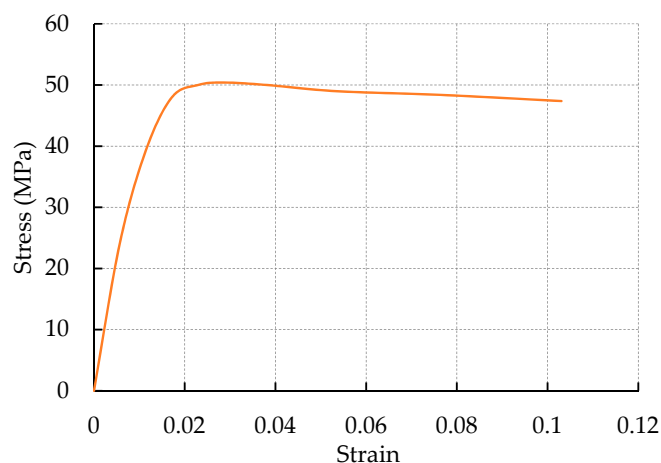


Figure 3. Stress-strain curve of uPVC under tensile load.

It was observed that the tensile properties of uPVC tube for samples that were taken from two pipes both perpendicular and parallel to the direction of extrusion have shown similar behavior (see Table 4). The percentage variations of strength, Young's Modulus of elasticity, and Poisson ratios are less than one percent (1%). The uPVC tube exhibited similar properties in all directions and, therefore, the uPVC tube is an isotropic material. Additionally, the result was compared with the values that were obtained from the literature. The physical properties of uPVC tube that were obtained from the literature are shown in Table 5, where the ultimate strength, Young's modulus, and Poisson's ratio ranged between 20.2–107 MPa, 2.52–4.03 GPa, and 0.34–419, respectively. The ultimate tensile strength values obtained from Gupta [7], Fakharifar [36], and Alves and Martins [1] resulted in a

percentage variance of less than 10% when compared to the experimental result. Similarly, the Young's modulus from Gupta [7] and Gathimba et al. [6], and the Poisson's ratio from Alves and Martins [1] and Chen et al. [37] resulted in a percentage variance of less than 10%. Figure 3 shows a sample representative stress-strain curve of uPVC under a tensile load.

Table 5. Physical property of uPVC pipe by other researchers.

Parameter	Ultimate Tensile Strength (MPa)	Young's Modulus (GPa)	Poisson Ratio
Gupta [7]	27.50–52.00	3.38	0.380
Gathimba et al. [6]	39.96	3.38	0.380
Fakharifar [36]	50.36	4.03	0.419
Alves and Martins [1]	54.00	2.45	0.340
Chen et al. [37]	107.00	2.52	0.360
Xue et al. [17]	20.20	3.08	-
Present study	49.74	3.58	0.342

The compressive load carrying capacity or strength of uPVC pipe is later required to compare the sum of individual load carrying capacity (concrete + uPVC) with that of the uPVC confined concrete cylinder. The compressive strength of empty uPVC tube was obtained by testing the hollow uPVC specimen under axial compression loads. The equivalent cylinder size specimen was prepared by cutting the uPVC into the required size, as shown in Figure 4 and tested using a UTM machine at a rate of 0.2 MPa/s.

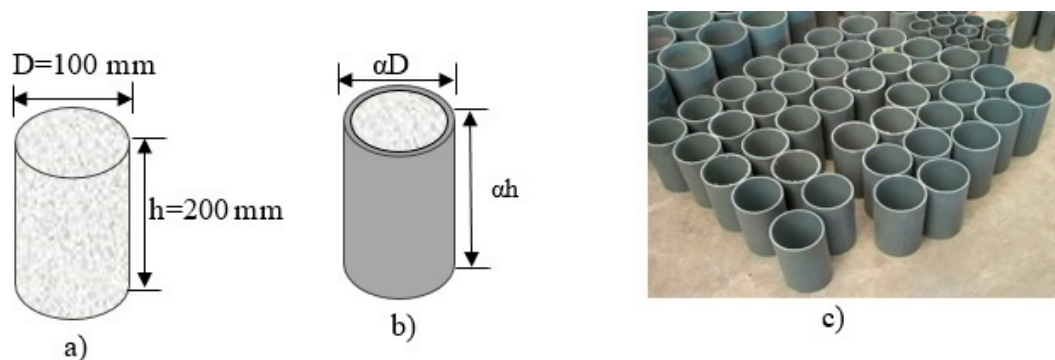


Figure 4. (a) Standard concrete cylinder size; (b) equivalent cylinder size uPVC pipe; and, (c) specimen prepared.

2.2. Concrete-Filled uPVC Tube Equivalent Cylinder ($h/D = 2$)

A total of 60 unconfined and 60 equivalent concrete-filled uPVC tube cylinders with different values of concrete compressive strength, w/c ratio, thickness to diameter ratio, and height to diameter ratio of two ($h/D = 2$) were prepared to investigate the compressive strength of both uPVC confined and unconfined concrete cylinders, as shown in Figures 5 and 6a. Figure 5 describes the matrix of variables the considered for the preparation of unconfined and uPVC confined concrete equivalent cylinders. The equivalent uPVC confined concrete cylinders were prepared by cutting a uPVC tube having different diameter $D = 63, 90, 110,$ and 140 mm through maintaining the height to diameter ratio at two ($h/D = 2$), as shown in Figure 4c. Five different compressive strength of concrete (cylinder/cube: C12/15, C16/20, C20/25, C25/30, and C28/35) were used to cast the cylinders. Concrete cubes (BS EN 12390-2:2009) [38], concrete cylinders (ASTM C39-12) [39], equivalent uPVC confined, and unconfined concrete cylinders were cast by filling the wet concrete mix in three layers and compacting until no bubbles were seen on the surface (BS EN 12390-2:2009) [38]. After 24 hours, the specimens were labeled based on concrete strength class (C1 = C12/15, C2 = C16/20, C3 = C20/25, C4 = C25/30, and C5 = C28/35), uPVC diameter (P1 = 63 mm, P2 = 90 mm, P3 = 110 mm, and P4 = 140 mm) and height to diameter

ratio ($H1 = (h/D = 2)$); thus, C1P1H1 means a confined concrete cylinder having a concrete strength of C12/15, uPVC diameter of 63 mm, and aspect ratio of two ($h/D = 2$). The specimens were cured in water for 28 days. At the 28th day, the specimens were brought out from water and the two sides of the confined cylinders were smoothed using a concrete cutting machine to avoid a local buckling of the uPVC tube at the edge, and allowed to dry prior to testing, as shown in Figure 6a. All of the specimens (confined and unconfined) were tested on the same day. The test was performed using Compression Machine, Servo-Plus Evolution Control Unit which has a capacity of 2000 kN, with load and displacement rate control system and a capacity to capture a measurement every 0.05 second. In addition, a load cell, transducers, and strain gages connected to TDS-630 Datalogger used to capture the measurements. Figure 6b shows the axial compression test setup. Placing two strain gauges on the specimens to measure axial and radial strains completed the instrumentation. The specimen was placed between the two flattens of the compression testing machine. Two LVDTs (linear variable differential transducers) were placed vertically, pointing to the moving plate of the machine to measure the axial deformation. Subsequently, the strain gauges, load cells, and LVDTs were connected to the TDS-630 data logger. The load was applied to the specimen at the rate of 0.2 MPa/s until failure. The data was recorded both from the compression machine (Load-time data, Max. Load, and Max. Strength) and TDS-630 Datalogger (time, Load, axial strain, radial strain, and displacement).

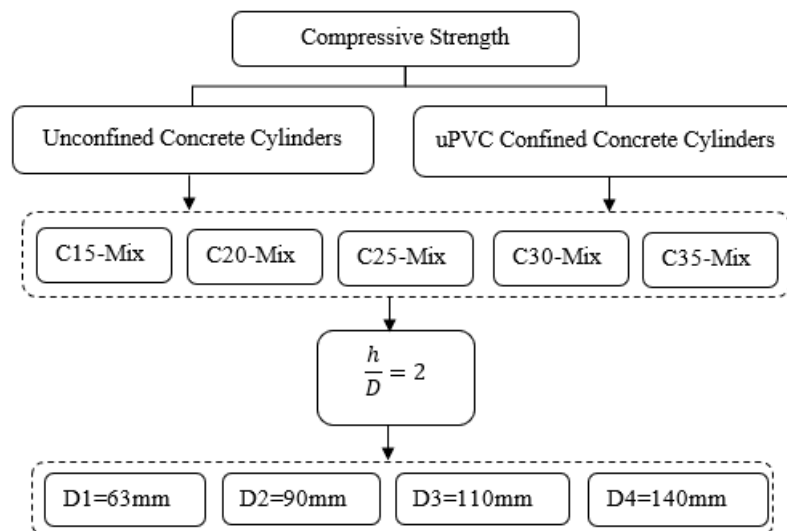


Figure 5. Matrix of variables considered for preparation of unconfined and uPVC confined concrete equivalent cylinders.

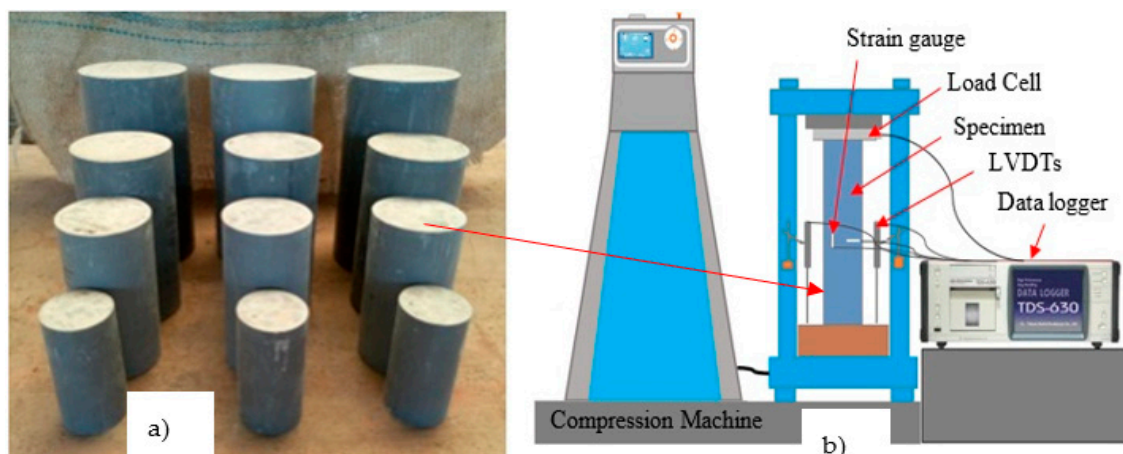


Figure 6. (a) uPVC confined concrete cylinders; (b) Test setup.

3. Results and Discussions

3.1. Load Carrying Capacity, Deformation and Specimen Behavior

The uPVC confinement in a uPVC confined concrete cylinder improved the load carrying capacity, as shown in Table 6. The uPVC confined concrete has shown superior performance when compared to the individual performance of uPVC and concrete combined. For different confinement to concrete ratios ($2t/D$), the load carrying capacity increased by 12–65%. The confinement performed well for lower concrete strength, increasing the load carrying capacity of up to 65%. uPVC confined the concrete specimens that were prepared from lower $2t/D$ ratio exhibited a post-peak displacement softening with a sudden strength loss. When the $2t/D$ ratio was increased from 0 to 0.079, the specimens exhibited a post-peak displacement softening and a ductile behavior without a sudden strength loss, as shown in Figure 7a. Similarly, specimens that were prepared from lower concrete class exhibited relatively better resistance at post-peak load when compared to the specimen that was prepared from higher concrete class, as shown in Figure 7b. For an equal cross-section of a specimen, the load carrying capacity increased as the confinement to concrete ratio increases.

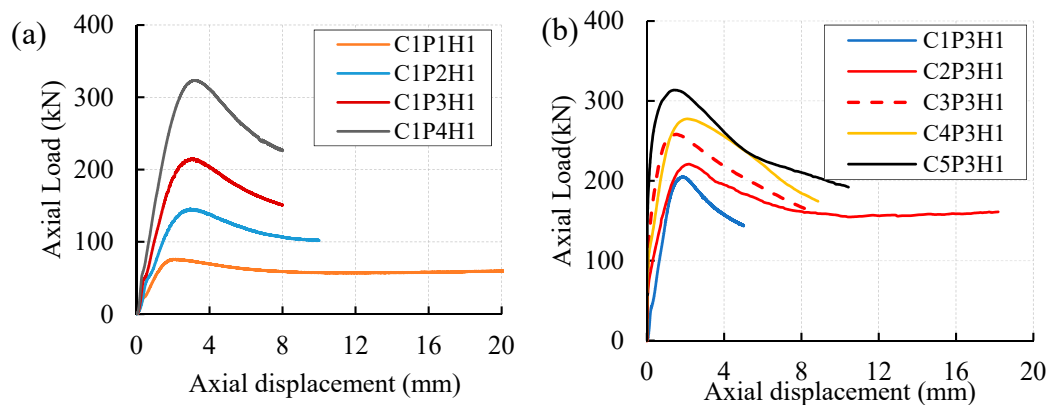


Figure 7. Load-displacement curve of uPVC confined concrete cylinders for: (a) different uPVC tube size; (b) Different concrete classes.

Generally, the uPVC confined concrete has undergone more than 4.7 mm axial deformation for all of the specimens at failure load which is by far more than the unconfined concrete deformation (<1 mm). Unlike unconfined concrete, the uPVC confined concrete has undergone high deformation after reaching a maximum load exhibiting high ductility. The deformations of all confined concrete cylinders from the peak to failure load were more than 53% of the total deformation and less than 19% for the unconfined concrete cylinder.

Table 6. Average Maximum Values of Load Carrying Capacity and Deformation.

Label	t (mm)	D (mm)	P _{CO} (kN)	P _{CC} (kN)	P _u (kN)	P _{CO+P_u} (kN)	$\frac{P_{CC}}{P_{CO+P_u}}$	Axial Deformation at Maximum Load (mm)	Axial Deformation at Failure Load (mm)	Max.Lateral Expansion at Failure Load (mm)
C1P1H1	2.5	63	30.17	75.99	16.02	46.18	1.65	2.0	27.0	23.6
C1P2H1	3	90	61.33	147.25	41.49	102.82	1.43	2.3	17.7	26.9
C1P3H1	3	110	98.31	209.07	49.01	147.32	1.42	3.0	8.0	11.8
C1P4H1	3	140	154.25	323.14	63.57	217.81	1.48	2.9	7.5	10.9
C2P1H1	2.5	63	40.22	85.63	16.02	56.24	1.52	2.1	6.0	8.4
C2P2H1	3	90	81.77	170.47	41.49	123.26	1.38	3.1	12.5	12.7
C2P3H1	3	110	131.08	235.69	49.01	180.08	1.31	3.5	12.5	12.5
C2P4H1	3	140	205.66	365.69	63.57	269.22	1.36	3.8	10.5	10.8
C3P1H1	2.5	63	49.26	89.53	16.02	65.27	1.37	1.8	5.6	12.2
C3P2H1	3	90	100.13	181.19	41.49	141.63	1.28	2.2	8.0	10.1
C3P3H1	3	110	160.52	256.50	49.01	209.53	1.22	2.2	4.7	8.4
C3P4H1	3	140	251.85	378.18	63.57	315.42	1.20	2.2	7.3	11.7
C4P1H1	2.5	63	58.71	100.14	16.02	74.73	1.34	1.8	9.9	14.0
C4P2H1	3	90	119.36	195.17	41.49	160.85	1.21	2.0	6.0	10.4
C4P3H1	3	110	191.34	281.85	49.01	240.35	1.17	1.9	6.6	9.8
C4P4H1	3	140	300.20	431.18	63.57	363.77	1.19	2.0	6.3	10.1
C5P1H1	2.5	63	70.34	108.25	16.02	86.35	1.25	1.5	5.9	8.3
C5P2H1	3	90	142.99	218.29	41.49	184.48	1.18	2.8	7.6	8.7
C5P3H1	3	110	229.22	311.38	49.01	278.23	1.12	2.2	6.9	14.4
C5P4H1	3	140	359.63	475.16	63.57	423.20	1.12	2.1	6.2	10.3

3.2. Failure Modes and Patterns

The main failure modes that were observed for uPVC confined concrete columns under axial load were a drum-type and shear-type failure, as shown in Figures 8 and 9. The hollow uPVC tube failed through buckling inward and outward under axial load. However, at a confined state, the uPVC was restrained by concrete from local buckling. Unlike steel, no local buckling of uPVC was seen at early stage loading due to the lower Young's modulus elasticity of uPVC. After the uPVC confined concrete column reaches the maximum load, the uPVC starts changing the color from grey to whitish grey at the middle of the specimen, and further develops bumps and strips on the surface. The color change was due to the yielding and elongation of the uPVC pipe. The two prevalent failure modes observed were drum and shear type failure, which were dependent on the failure mode the concrete's core. The drum type failure occurred due to the expansion of concrete's core at the middle resulting from cone type failure. The shear-type failure occurred due to shear failure of the concrete's core. The uPVC along and around the crack of concrete's core has undergone color change, which shows significant elongation and plastic deformation around the cracked region. In addition to the color change, the specimen developed a pump along the direction of the crack. Further loading the specimen that is undergoing a shear-type failure created folds on the uPVC pipe creating elephant foot type structure.



Figure 8. Drum Type Failure.



Figure 9. Shear Type Failure.

3.3. Confinement Effectiveness

The confinement effectiveness is the measure of how the uPVC pipe confines the concrete. It is the ratio of uPVC confined concrete strength to the unconfined concrete strength (f_{cc}/f_{co}) and it is affected by the concrete's core strength, the $2t/D$ ratio and the tensile strength of uPVC pipe. As shown in Table 7 and Figure 10, an increase in the $2t/D$ ratio of a uPVC confined concrete specimen improved the strength enhancement ratio (f_{cc}/f_{co}) and the ultimate strength. The strength enhancement ratio

(f_{cc}/f_{co}) increased as the concrete strength decreased and vice versa. Maintaining a uPVC diameter as 63mm ($2t/D = 0.079$) and changing the concrete classes from C15 to C35 decreased the strength enhancement ratio from 2.35 to 1.44. Similarly, for the uPVC size of 90, 110, and 140 mm, the strength enhancement ratio decreased from 2.23 to 1.42, 2.12 to 1.36, and 2.03 to 1.28, respectively, for the concrete strength classes used from C15 to C35. Similar researches that were done by Oyawa et al. [5] showed that the strength enhancement ratio ranged in between 1.18 and 3.65 for different concrete strength and pipe size.

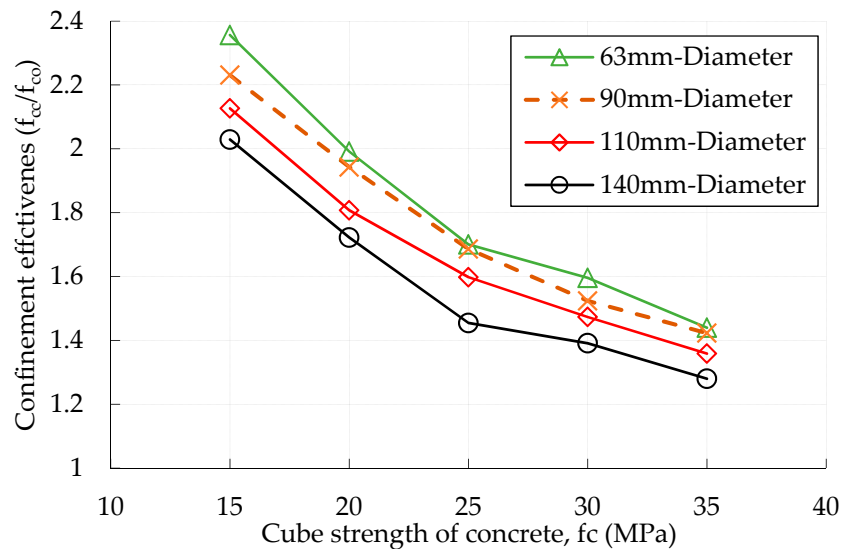


Figure 10. The effectiveness of uPVC confinement.

Table 7. Average Maximum Strength, Strain, Confinement Contribution, Energy absorption, Work Index, and Ductility Factor.

Label	D (mm)	t (mm)	f_{co} (MPa)	f_{cc} (MPa)	ϵ_{co} (mm/mm)	ϵ_{cc} (mm/mm)	ϵ_1 (mm/mm)	ϵ_{cr} (mm/mm)	f_{cc}/f_{co}	$\epsilon_{cc}/\epsilon_{co}$	f_l (MPa)	k_1	μ_{cr}	E (MJ/m ³)	W_{cr}	$\frac{E_c}{E_u}$
C1			10.35		0.0021		0.0014	0.0024					1.803	0.019	2.650	1.000
C1P1H1	63	2.5		24.38		0.0183	0.01	0.1335	2.356	8.946	4.397	3.192	13.350	4.499	36.915	243.145
C1P2H1	90	3		23.08		0.0137	0.0095	0.056	2.231	6.699	3.643	3.496	5.895	1.274	11.617	68.820
C1P3H1	110	3		22.00		0.0153	0.008	0.03725	2.127	7.458	2.942	3.961	4.656	0.608	6.910	32.862
C1P4H1	140	3		20.99		0.0107	0.008	0.0265	2.029	5.234	2.284	4.662	3.313	0.460	5.474	24.840
C2			13.79		0.0026		0.0016	0.0029					1.790	0.028	2.509	1.000
C2P1H1	63	2.5		27.47		0.0133	0.0085	0.065	1.992	5.217	4.397	3.111	7.647	1.221	10.461	44.113
C2P2H1	90	3		26.80		0.0181	0.008	0.146	1.943	7.115	3.643	3.570	18.250	3.134	29.235	113.192
C2P3H1	110	3		24.93		0.0184	0.0095	0.13	1.808	7.216	2.942	3.786	13.684	1.779	15.023	64.264
C2P4H1	140	3		23.76		0.0147	0.0090	0.04	1.722	5.778	2.284	4.363	4.444	0.636	5.951	22.980
C3			16.89		0.0029		0.0017	0.0033					1.896	0.038	2.620	1.000
C3P1H1	63	2.5		28.72		0.0138	0.0055	0.056	1.700	4.826	4.397	2.691	10.182	1.230	15.570	32.217
C3P2H1	90	3		28.48		0.0161	0.00525	0.0745	1.686	5.635	3.643	3.181	14.190	1.744	23.334	45.698
C3P3H1	110	3		26.99		0.0098	0.00325	0.0515	1.598	3.433	2.942	3.432	15.846	1.138	25.949	29.815
C3P4H1	140	3		24.57		0.0094	0.005	0.065	1.454	3.316	2.284	3.361	13.000	1.110	18.066	29.067
C4			20.13		0.0031		0.0019	0.0035					1.885	0.054	2.884	1.000
C4P1H1	63	2.5		32.13		0.0159	0.004	0.1155	1.596	5.227	4.397	2.727	28.875	3.122	48.599	58.137
C4P2H1	90	3		30.68		0.0221	0.0065	0.104	1.524	7.239	3.643	2.895	16.000	2.465	24.720	45.890
C4P3H1	110	3		29.66		0.0129	0.006	0.065	1.473	4.225	2.942	3.238	10.833	1.477	16.602	27.507
C4P4H1	140	3		28.01		0.0072	0.0035	0.031	1.391	2.373	2.284	3.449	8.857	0.634	12.933	11.804
C5			24.12		0.0033		0.0020	0.0037					1.849	0.064	2.634	1.000
C5P1H1	63	2.5		34.73		0.0097	0.0035	0.0645	1.440	2.983	4.397	2.412	18.429	1.556	25.613	24.497
C5P2H1	90	3		34.31		0.0154	0.007	0.058	1.423	4.726	3.643	2.798	8.286	1.460	12.161	22.987
C5P3H1	110	3		32.77		0.0118	0.0045	0.05475	1.358	3.640	2.942	2.939	12.167	1.419	27.834	32.297
C5P4H1	140	3		30.87		0.0080	0.00325	0.037	1.280	2.451	2.284	2.955	11.385	0.697	13.894	10.968

3.4. Effect of Thickness to Diameter ($2t/D$)

As shown in Figure 11a–c,e), the strength of uPVC confined concrete equivalent cylinder increased as the $2t/D$ ratio increases. The thickness to diameter ratio affected the post-peak behavior of the stress-strain or load-displacement curve (see Figure 7a). The absolute value of the slope of the post-peak curve decreased as the thickness to diameter ratio increases. To relate the effect of the $2t/D$ ratios on the strength of uPVC confined concrete equivalent cylinders, the following equations were derived through a linear regression for different classes of concrete. The average unconfined concrete cylinder strength (f_{co}) for different classes of concrete (cube strength) are given as f_{co}^{class} and f_{cc}^{class} for the confined. Accordingly, the five classes of concrete used in this research are C15 (C1), C20(C2), C25(C3), C30(C4), and C35(C5).

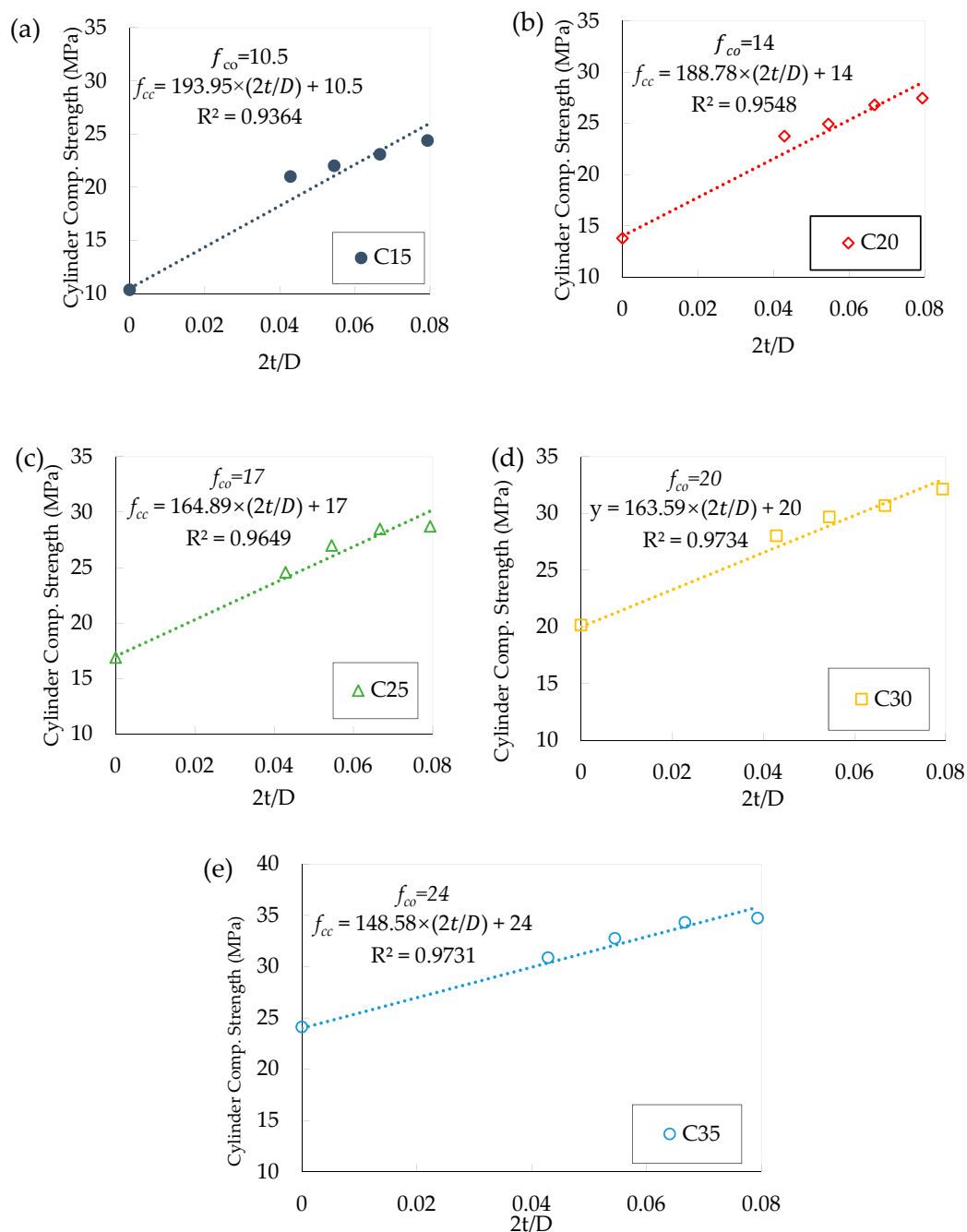


Figure 11. Effect of thickness to diameter ratio ($2t/D$) on strength of uPVC confined concrete for: (a) C15, (b) C20, (c) C25, (d) C30, and (e) C35.

For the C15(C1) concrete class, the approximate average unconfined concrete cylinder strength is 10.35 MPa and the confined strength was related with the unconfined one for different $2t/D$ ratios are expressed, as follows, in Equation (2).

$$f_{cc}^{C1} = 193.95\left(\frac{2t}{D}\right) + f_{co}^{C1} \quad (2)$$

Similarly, the uPVC confined concrete strength for concrete classes of C20, C30, C30, and C35 are given, as follows Equations (3)–(6)

$$f_{cc}^{C2} = 188.7\left(\frac{2t}{D}\right) + f_{co}^{C2} \quad (3)$$

$$f_{cc}^{C3} = 164.89\left(\frac{2t}{D}\right) + f_{co}^{C3} \quad (4)$$

$$f_{cc}^{C4} = 163.59\left(\frac{2t}{D}\right) + f_{co}^{C4} \quad (5)$$

$$f_{cc}^{C5} = 148.58\left(\frac{2t}{D}\right) + f_{co}^{C5} \quad (6)$$

Based on Figure 11, the slope of the curve is dependent on the strength of the concrete. The slopes in Equations (3)–(6) are dependent on the strength of concrete. Thus, a relation was developed between the slopes of Equations (3)–(6) (193.95, 188.7, 164.89, 163.59, and 148.58) and concrete cylinder strength values (10.35, 13.79, 16.89, 20.13, and 24.12), where $Slope = 432 / f_{co}^{0.331}$.

Based on the above relations, the general equation (Equation (7)), which represents a uPVC confined concrete strength as a function of concrete strength, uPVC tube diameter and thickness was developed. The relations developed in Figure 11 were used to predict the confined concrete strength for different concrete classes and $2t/D$ ratios and they are tabulated in Table 8.

$$f_{cc} = f_{co} + \left(\frac{432}{f_{co}^{0.331}}\right) \times \left(\frac{2t}{D}\right) \quad (7)$$

Table 8. Predicted strength for different concrete classes and $2t/D$ ratios.

Concrete Class	$2t/D$	Cylinder Strength (MPa) (f_{cc})	Determination Coefficient (R^2)	Correlation Coefficient (R)
C15	0	10.50	0.936	0.967
	0.043	18.81	0.936	0.967
	0.055	21.08	0.936	0.967
	0.067	23.43	0.936	0.967
	0.079	25.89	0.936	0.967
C20	0	14.00	0.955	0.977
	0.043	22.09	0.955	0.977
	0.055	24.30	0.955	0.977
	0.067	26.59	0.955	0.977
	0.079	28.98	0.955	0.977
C25	0	17.00	0.965	0.982
	0.043	24.07	0.965	0.982
	0.055	25.99	0.965	0.982
	0.067	27.99	0.965	0.982
	0.079	30.09	0.965	0.982
C30	0	20.00	0.973	0.986
	0.043	27.01	0.973	0.986
	0.055	28.92	0.973	0.986
	0.067	30.91	0.973	0.986
	0.079	32.98	0.973	0.986
C35	0	24.00	0.973	0.986
	0.043	30.37	0.973	0.986
	0.055	32.10	0.973	0.986
	0.067	33.91	0.973	0.986
	0.079	35.79	0.973	0.986

3.5. Effect of Core Concrete Strength and Pipe Size

The uPVC confinement increased the strength for all five classes of concrete that were used in this research; however, it has shown a decreasing rate as the concrete strength increased. Figures 12 and 13 shows the effect of concrete strength and pipe size on the axial compressive strength of uPVC tube confined concrete cylinders. The strength increased by an average value of 13% as the pipe diameter decreases from 140 to 63 mm. As the diameter of the pipe decreases, the $2t/D$ ratio increases and the strength also increases with $2t/D$ ratio. For concrete that was confined by the 63 mm diameter of uPVC tube, the strength increased by 135, 99, 70, 59, and 43% for the concrete strength classes of C15, C20, C25, C30, and C30, respectively. Similarly, for a uPVC size of 90, 110, and 140 mm, the strength increased by 123, 94, 68, 52, and 42%, 113, 80, 60, 47, and 37% and 103, 72, 45.5, 40, and 28%, respectively, for the above concrete strength classes.

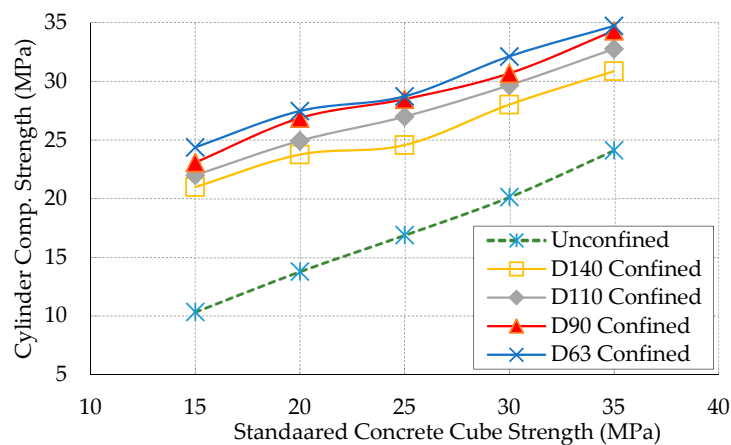


Figure 12. Effect of concrete classes on the strength of uPVC confined concrete cylinders.

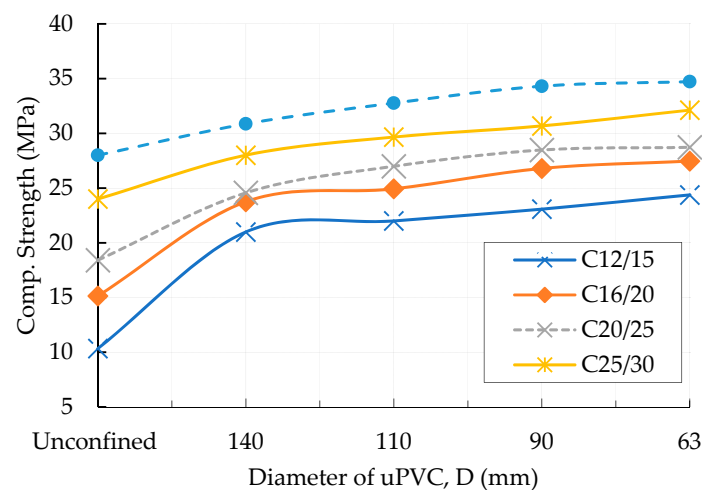


Figure 13. Effect of pipe diameter on strength of uPVC confined concrete cylinders.

3.6. Stress-Strain Relation

The unconfined concrete compression test was done on cylinders that were made from different diameters (63, 90, 100, 110, and 140) through maintaining height to diameter ratio to two ($h/D = 2$). The result has shown that there is no variation on strength and stress-strain behavior due to the size of the cylinder that has the same height to diameter ($h/D = 2$). Figure 14 shows the unconfined stress-strain curve that was drawn from two sample specimens for each class of concrete. The maximum strain recorded at a failure load is 0.00376. The specimens failed very fast after reaching the peak strength. The strain from the peak stress to the failure stress was less than 19% of the total strain.

Figures 15a–e and 16a–d shows the stress-strain curve of the uPVC confined concrete equivalent cylinders. The stress-strain curves were plotted for different classes of concrete and uPVC tube diameters (for different $2t/D$ ratios). The strain significantly improved, which is more than 0.1 for some specimens when compared to the maximum unconfined failure strain (0.00376). It was observed that there was a sudden drop in stress after reaching the peak strength for lower $2t/D$ ratio (large diameter of uPVC tube). The pipe diameter (or $2t/D$ ratio) significantly affected the post-peak behavior of uPVC confined equivalent cylinders. The equivalent uPVC confined concrete cylinder with higher $2t/D$ ratio has shown a gradual drop in the stress-strain curve after reaching the peak strength, and the specimen with lower $2t/D$ ratio exhibited a sudden drop.

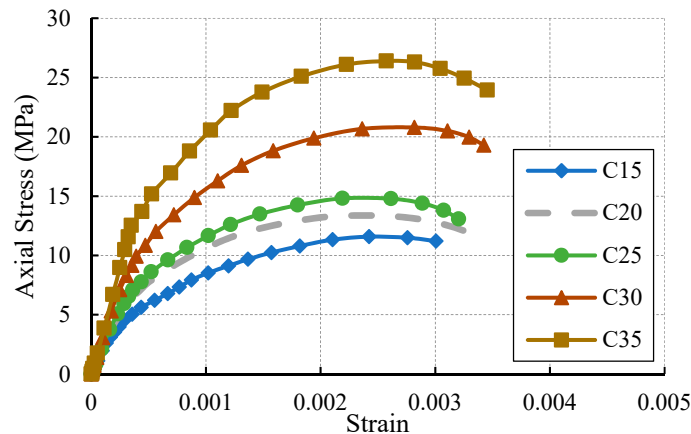


Figure 14. Stress-Strain curve of the unconfined concrete cylinder of C15 to C35.

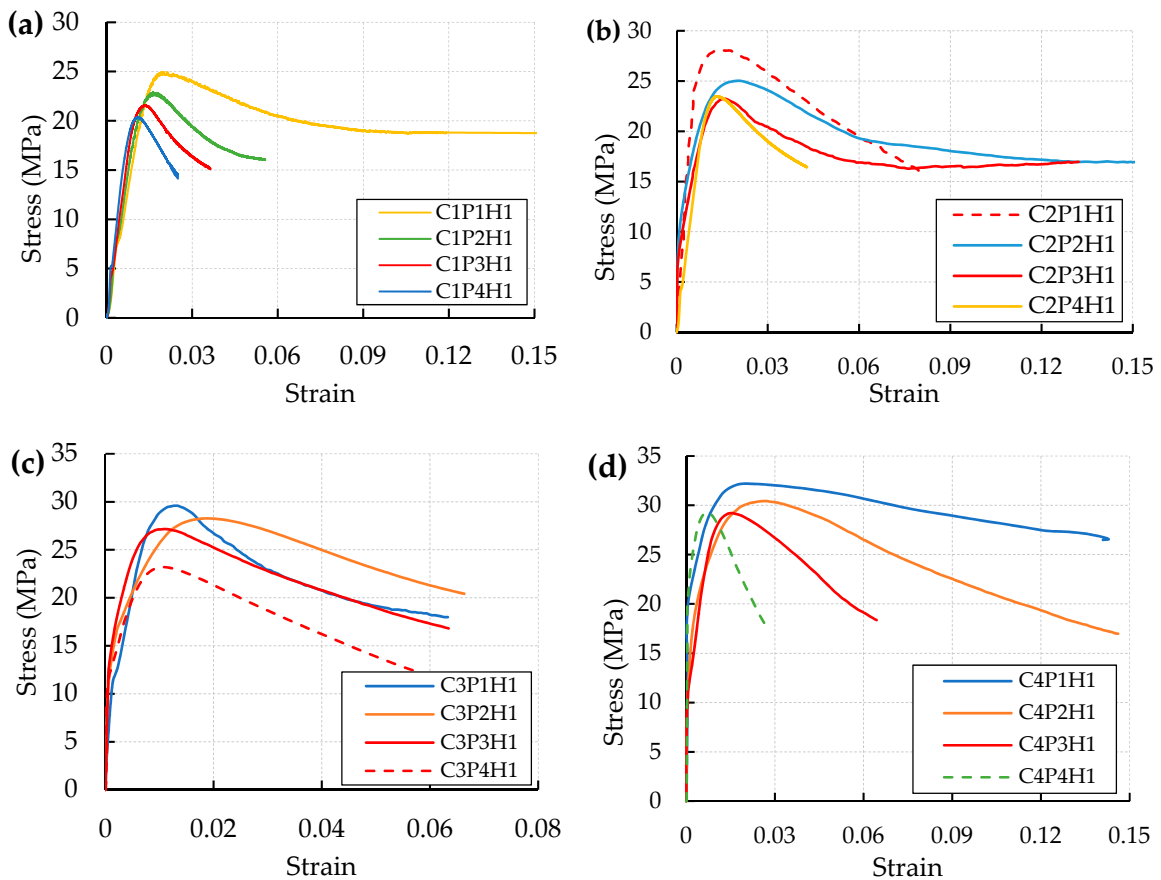


Figure 15. Cont.

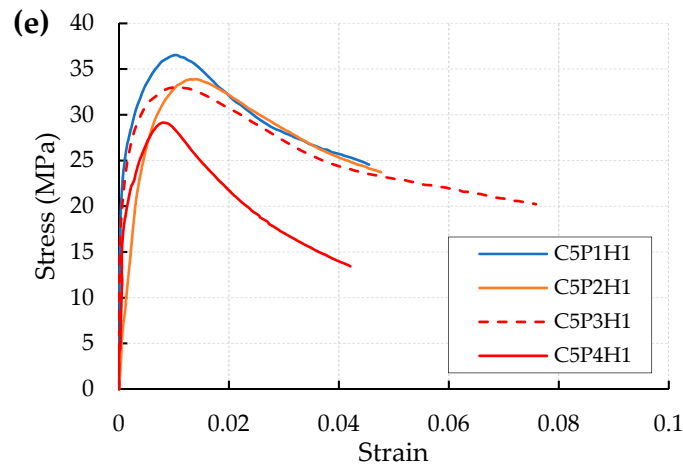


Figure 15. Stress-Strain curve of different uPVC tube size confined concrete cylinder for: (a) C15, (b) C20, (c) C25, (d) C30, and (e) C35.

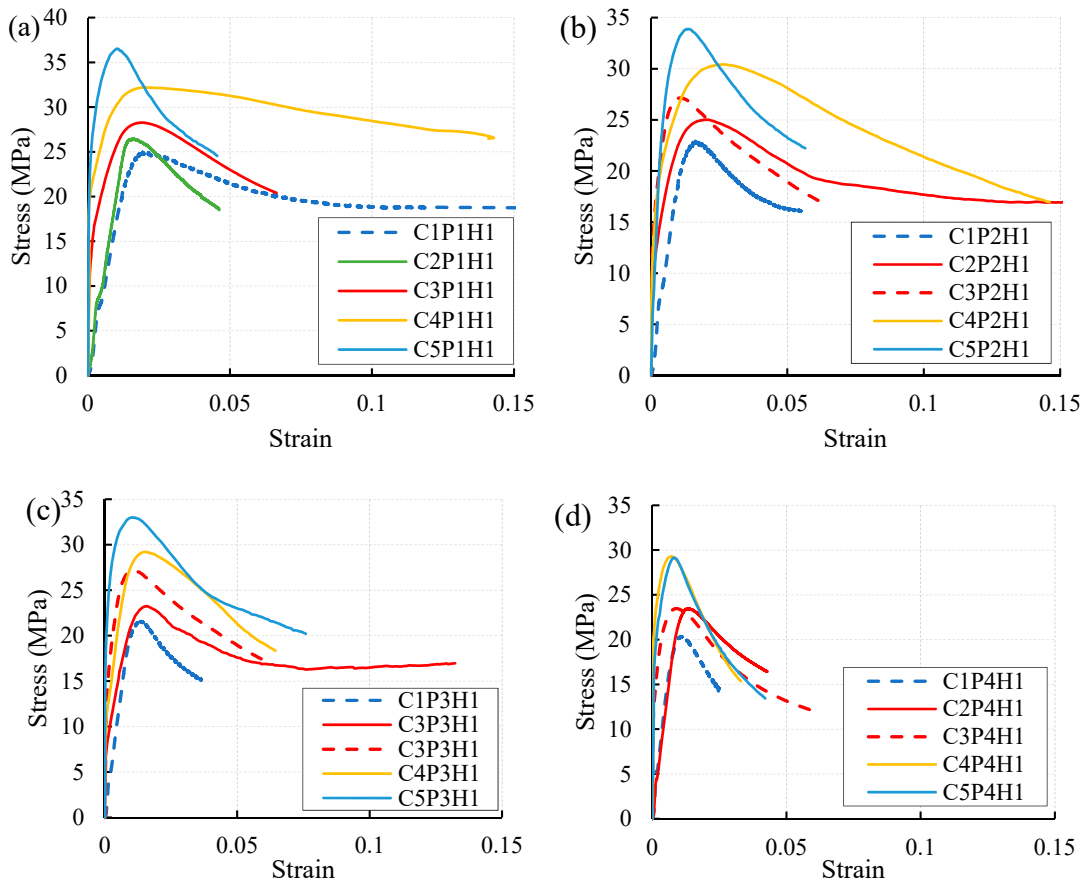


Figure 16. Stress-Strain curve of different classes of concrete filled uPVC tube cylinders for uPVC size of: (a) 63 mm, (b) 90 mm, (c) 110 mm, and (d) 140 mm.

3.6.1. Ductility Factor

The ductility factor is the ratio of fracture strain (or strain at inelastic yield strength demand) to strain at elastic maximum strength [40–43]. Both the unconfined and confined ductility factors were calculated while using the expression given in Equation (8) and stress-strain response parameters on the curve in Figure 17.

$$\mu_{cf} = \frac{\epsilon_{cr}}{\epsilon_1} \tag{8}$$

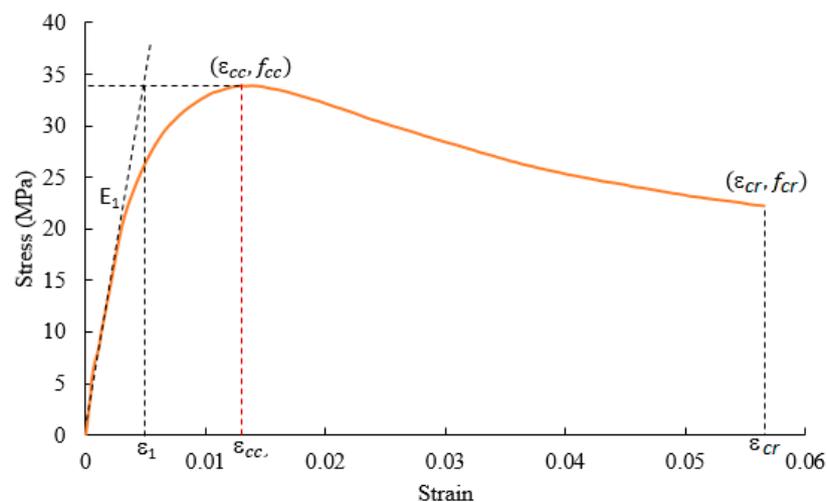


Figure 17. Stress-strain response parameters used to calculate the ductility factor.

Figure 18 presents the ductility factor for the unconfined and uPVC confined concrete specimens. The ductility factor increased from 1.84 to 28.75 as the $2t/D$ ratio increases from 0 to 0.79. The uPVC confined concrete specimens experienced post-peak strain softening without sudden strength loss when compared to the unconfined specimens. Under axial compression, the unconfined concrete suddenly lost the resistance and then ruptured into pieces after reaching the peak strength. For confined specimens, the uPVC confinement significantly contributed to ductility by delaying the development of concrete cracks and volume expansion.

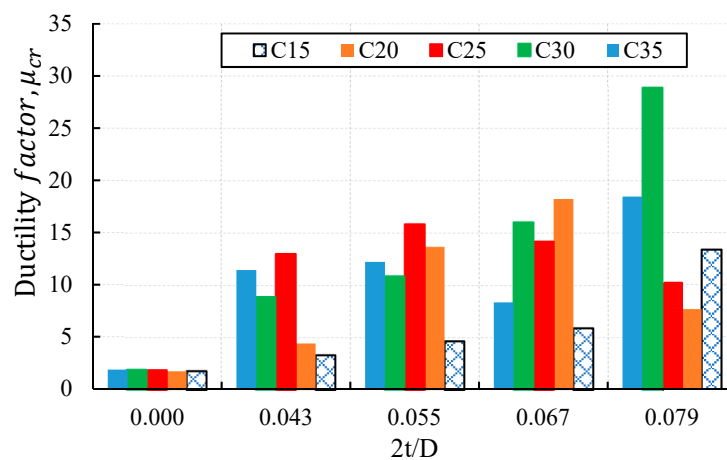


Figure 18. Ductility factor for different concrete classes and $2t/D$ ratios.

3.6.2. Energy Absorption Capacity

Energy absorption is the toughness of the material, as measured from the stress-strain data. It is the area under a stress-strain curve and is measured using the expression that is given in Equation (9). On literature, energy absorption was reported in different ways depending on the strain value that was chosen to end the integration [15,40,42–44]. In this study, the energy absorption per volume at 100% strain (ultimate toughness) was calculated for both confined and unconfined equivalent specimens, as shown in Table 6. To facilitate the calculation, OriginPro data analysis software was used to calculate the area under the stress-strain curve, as shown in Figure 19.

$$E = \iint d\sigma d\varepsilon \quad (9)$$

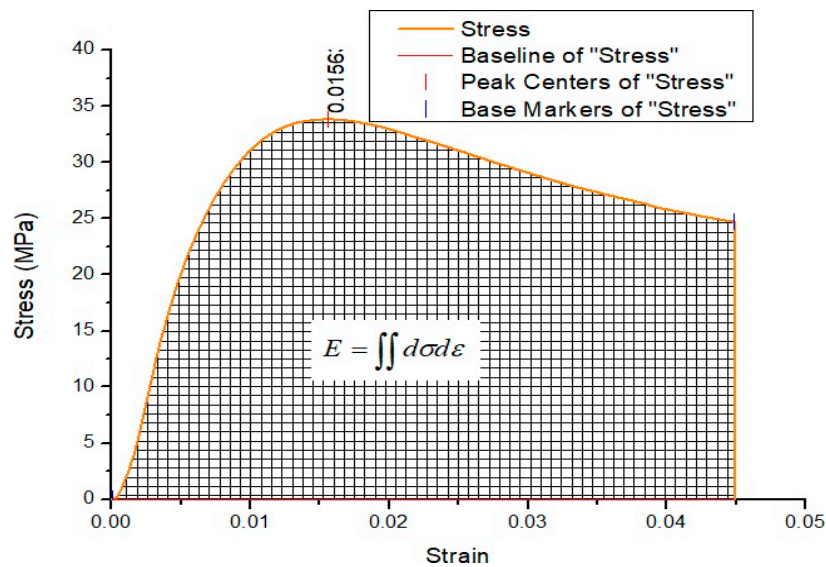


Figure 19. The area under stress-strain curve using OriginPro.

The uPVC confinement increased energy absorption capacity of the confined concrete. Overall, the ratio of the confined to unconfined energy absorption per volume (E_C/E_U) increased from 10.968 to 243.145. Apart from the irregularities on some values, the energy absorption increased as the $2t/D$ value increased. As is shown in Figure 20, the energy absorption capacity is much influenced by the uPVC thickness and diameter. Therefore, it was anticipated that the uncertainties of these parameters have caused irregularities on the result.

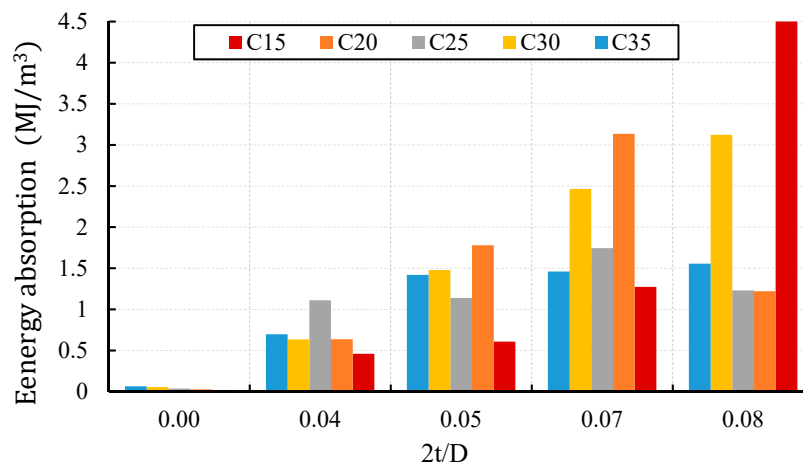


Figure 20. Energy absorption capacity for different concrete classes and $2t/D$ ratios.

3.6.3. Work Index

Work is a total force required to shorten the uPVC confined cylinder under axial compression and it is stored as energy in the material. Energy stored in the material is the area under the stress-strain curve, as expressed in Equation (9) and Figure 20. The work index is calculated to show how the material undergoes straining for the applied load beyond the elastic state. The work index was calculated as the ratio of the total area under the stress-strain curve to the area of the stress-strain curve under the elastic region, and it is expressed in Equation (10).

$$W_{cr} = \frac{E}{E_1} = \frac{E}{\frac{1}{2}(f_{cc} \times \varepsilon_1)} = \frac{2E}{(f_{cc} \times \varepsilon_1)} \quad (10)$$

Apart from increasing the strength and ductility, the uPVC confinement improved the energy absorption and load carrying capacity of the confined concrete at the inelastic state (see Table 7). The confinement helped the specimen to stay for a prolonged period of time without failure after reaching the maximum load as compared to the unconfined specimen. The calculated work index parameter ranged from 10.97 to 48.599 for the uPVC confined and 2.65 to 2.884 for the unconfined specimens, as shown in Table 7.

3.7. Analytical Equations on Peak Strength and Strain

The analytical expression for the confined concrete that relates the concrete strength, tensile strength, thickness, and diameter of the confining material in Equation (11) was developed for the first time in 1928 [45]. Many researchers, for different types of confining materials, later modified this expression. The peak strength of the concrete-filled uPVC tube column is dependent on the uPVC thickness to diameter ratio (see Figure 11), tensile strength of the uPVC tube, and concrete strength (see Figure 12). For a circular cross-section, the lateral confining pressure is uniformly distributed on the perimeter.

In Table 7, the effectiveness of uPVC confinement in a uPVC confined concrete cylinder was calculated by dividing the experimental value of the confined concrete strength to the unconfined. However, the confined concrete strength is a function of the unconfined strength, uPVC thickness, diameter, and tensile strength of the uPVC pipe, as shown in Figure 21. Thus, the analytical expression for the uPVC tube confined concrete that relates the concrete strength, tensile strength, diameter, and thickness of the confining material, was developed based on Equation (11) and Equation (12).

$$f_{cc} = f_{co} + k_1 f_l \quad (11)$$

$$f_l = \frac{2t \times f_y}{(D - 2t)} \quad (12)$$

where:

f_l —lateral confining pressure;

f_y —tensile strength of uPVC tube;

k_1 —the confinement coefficient;

D —the diameter of confined cylinder; and,

t —the thickness of the uPVC tube as shown in Figure 21.

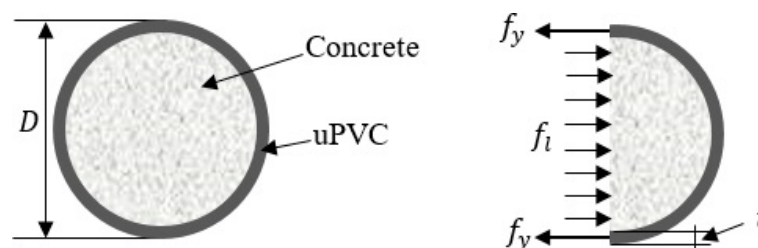


Figure 21. Lateral Confining Pressure.

As shown in Table 7, the value of k_1 decreased as the concrete strength increased; and increased as the $2t/D$ ratio decreased. Thus, k_1 is dependent on both the concrete strength (f_{co}) and $2t/D$ ratio, and the expression was developed using the experimental results to relate the parameters in Equation (13).

$$k_1 = \frac{2.7}{(f_{co})^{0.394} (2t/D)^{0.453}} \quad (13)$$

Substituting Equation (13) to Equation (11), the axial strength of uPVC tube confined concrete can be expressed in Equation (14).

$$f_{cc} = f_{co} + \frac{2.7f_l}{(f_{co})^{0.394}(2t/D)^{0.453}} \quad (14)$$

The strain at peak strength of concrete-filled uPVC tube column is dependent on the lateral confining pressure and concrete strength. The expression in Equation (15) was developed based on the experimental results in Table 7.

$$\varepsilon_{cc} = \varepsilon_{co} + 0.043\left(\frac{f_l}{f_{co}}\right)^{0.89} \quad (15)$$

Six existing and the new models in Table 9 are used to predict the peak strength (f_{cc}) and strain (ε_{cc}) of uPVC confined concrete columns and compared against the obtained experimental results. The accuracy of the model was evaluated using an average absolute error (AAE), as defined in Equation (16).

$$AAE = \frac{\sum_{i=1}^N \left| \frac{\text{Model}_i - \text{Exp}_i}{\text{Exp}_i} \right|}{N} \times 100 \quad (16)$$

Table 9. Models used for calculation of f_{cc} and ε_{cc} and their average absolute error (AAE) values.

Source	Peak Strength (f_{cc})	AAE (%)	Strain	AAE (%)
Cusson and Paultre [48]	$f_{cc} = f_{co} + 2.1f_{co}\left(\frac{f_l}{f_{co}}\right)^{0.7}$	7.4	$\varepsilon_{cc} = \varepsilon_{co} + 0.21\left(\frac{f_{cc}}{f_{co}}\right)^{1.7}$	48.0
Sastcioglu and Razvi [46]	$f_{cc} = f_{co} + 6.7(f_l)^{0.83}$	26.0	$\varepsilon_{cc} = \varepsilon_{co}\left(1 + 5\frac{f_l}{f_{co}}\right)$	57.5
Richart et al. [45]	$f_{cc} = f_{co} + 4.1f_l$	10.6	$\varepsilon_{cc} = \varepsilon_{co}\left(1 + 20.5\frac{f_l}{f_{co}}\right)$	19.3
Benzaid et al. [49]	$f_{cc} = f_{co}\left[1 + 2.2\left(\frac{f_l}{f_{co}}\right)\right]$	13.1	$\varepsilon_{cc} = \varepsilon_{co}\left(2 + 7.6\frac{f_l}{f_{co}}\right)$	29.3
Bisby et al. [47]	$f_{cc} = f_{co} + 3.587(f_l)^{0.84}$	5.3	$\varepsilon_{cc} = \varepsilon_{co} + 0.024\frac{f_l}{f_{co}}$	41.1
Xiao et al. [50]	$f_{cc} = f_{co}\left[1 + 3.24\left(\frac{f_l}{f_{co}}\right)^{0.8}\right]$	13.9	$\varepsilon_{cc} = \varepsilon_{co}\left(1 + 17.4\left(\frac{f_l}{f_{co}}\right)^{1.06}\right)$	21.4
Present study	$f_{cc} = f_{co} + \frac{2.7f_l}{(f_{co})^{0.394}(2t/D)^{0.453}}$	1.8	$\varepsilon_{cc} = \varepsilon_{co} + 0.043\left(\frac{f_l}{f_{co}}\right)^{0.89}$	16.7

Figures 22 and 23 compares the predicted peak strength and strain with the test results. Table 9 also presents the models and AAE of the predicted peak strength and strain value of uPVC confined concrete specimens. The proposed strength and strain models performed well with AAE of 1.8 and 16.7%, respectively, when compared with the existing models (see Table 9). All of the strength models, except Sastcioglu and Razvi [46], predicted the peak strength reasonably well with an AAE of less than 20%. The model by Bisby et al. [47] and Cusson and Paultre [48] predicted the peak strength accurately with an AAE of 5.3 and 7.4%, respectively. The proposed strain model predicted the strain reasonably well with an AAE of 16.7%. The strain models by Cusson and Paultre [48], Sastcioglu and Razvi [46], and Bisby et al. [47] predicted the strain less accurately with an AAE of more than 40%, and the Richart et al. [45], Benzaid et al. [49], and Xiao et al. [50] models predicted the strain with an AAE of less 30%.

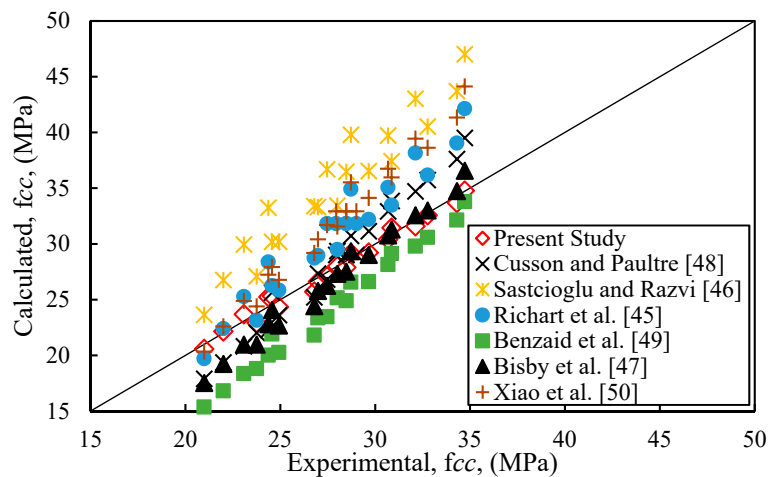


Figure 22. Performance of various confinement models in predicting the peak strength.

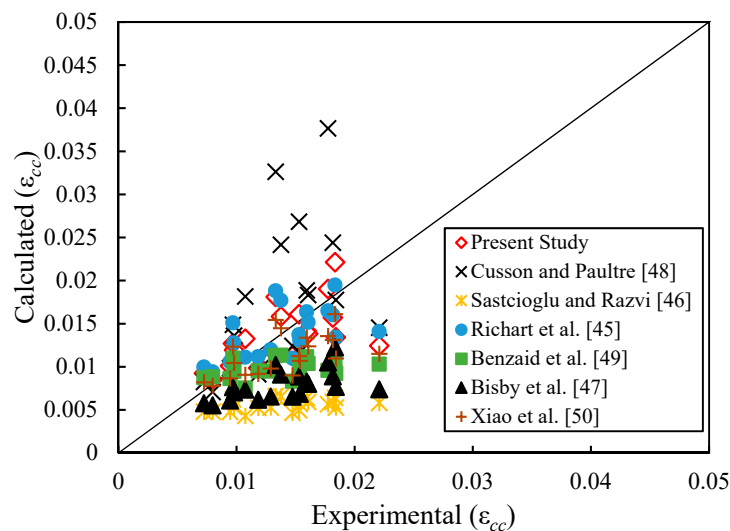


Figure 23. Performance of various confinement models in predicting strain at peak strength.

4. Conclusions

In this research, the experimental work on uPVC confined concrete equivalent cylinder was done to study the suitability and the performance of uPVC confined concrete columns for structural use. Based on the experiments that were carried out and the results regarding load carrying capacity, strength, ductility, energy absorption, failure mode, and post-peak behavior, the following conclusions are made:

- The uPVC tube in a uPVC confined concrete equivalent cylinder significantly contributed to the axial load carrying capacity. The load carrying capacity at the confined state was 1.12–1.65 times the sum of individual carrying capacity at unconfined state. Unlike unconfined concrete, which undergoes a brittle failure after reaching a maximum load, uPVC confined concrete showed high deformation after reaching a maximum load exhibiting a ductile failure.
- The uPVC confined concrete cylinder exhibited a ductile failure with high axial deformation. The two prevalent failure modes observed were drum and shear type failure, which are dependent on the failure mode of the core concrete. The drum type failure occurred due to the expanding of core concrete at the middle from cone type failure, whereas the shear-type failure occurred due to shear failure of the core concrete.

- The uPVC tube in a uPVC confined concrete increased the strength by 1.28–2.35 times the unconfined equivalent concrete cylinder. The effectiveness of the confinement was dependent on the core concrete strength and the 2t/D ratio. The effectiveness increased as the core concrete strength decreases and the 2t/D ratio increases.
- The post-peak stress-strain behavior of uPVC confined concrete proved to be affected by the 2t/D ratio. The absolute value of the slope decreased as the 2t/D ratio increased.
- The uPVC confinement in uPVC confined concrete cylinder increased both the ductility and energy absorption. The ductility factor and energy absorption increased by 1.84–15.3 and 11–243 times of the equivalent unconfined concrete cylinder, respectively. The confinement helped the specimen to stay for a prolonged period of time without failure after reaching the maximum load. In addition, the uPVC confinement helped the material to undergo straining beyond the elastic state without failure for a prolonged period of time when compared to the unconfined concrete cylinder.

To further understand the performance of the uPVC confined concrete column, additional tests should be done on different aspect ratios and under lateral and cyclic load. Even though uPVC is incombustible and self-extinguishing, it starts losing its stiffness when the temperature goes above 70 °C. Therefore, an innovative fire protection mechanism will facilitate the incorporation of uPVC confined concrete in the construction industry.

Author Contributions: Conceptualization, A.M.W., W.O.O. and T.N.; Methodology, A.M.W., W.O.O. and T.N.; Experiment and data collection, A.M.W.; software, A.M.W.; Analysis, A.M.W.; writing-original draft preparation, A.M.W.; writing-review and editing, A.M.W., W.O.O. and T.N.; funding acquisition, A.M.W., W.O.O. and T.N.

Funding: The authors sincerely thank the African Union Commission (AUC) and Africa-ai-Japan Project for funding this research.

Conflicts of Interest: The authors declare no conflict of interest.

Nomenclature

E	Energy Absorption Capacity	f_{co}	Unconfined compressive strength
uPVC	Unplasticized polyvinyl chloride	f_{cc}	Confined compressive strength
t	Thickness	W_{cr}	Work index
RC	Reinforced concrete	P_u	uPVC tube Load-carrying Capacity
PVC	Polyvinyl chloride	P_{co}	Unconfined Load carrying capacity
h	height	P_{co}	Confined load carrying Capacity
FRP	Fiber reinforced polymer	E_u	unconfined concrete energy absorption capacity
D	Diameter	E_c	Confined concrete energy absorption capacity
σ_1, σ_2 and σ_3	Principal stresses	ϵ_{cr}	Strain at failure load
μ_{cr}	Ductility factor	ϵ_{co}	strain at max strength of Unconfined concrete
k_1	Confinement Coefficient	ϵ_{cc}	strain at max strength of Confined concrete
f_y	Yield stress of uPVC	ϵ_1	Elastic strain at max strength
f_l	Lateral confining pressure		

References

1. Alves, L.M.; Martins, P.A.F. Cold expansion and reduction of thin-walled PVC tubes using a die. *J. Mater. Process. Technol.* **2009**, *209*, 4229–4236. [[CrossRef](#)]
2. Abdulla, N.A. Concrete filled PVC tube: A review. *Constr. Build. Mater.* **2017**, *156*, 321–329. [[CrossRef](#)]
3. Oyawa, W.O.; Gathimba, N.K.; Geoffrey, N.M. Innovative composite concrete filled plastic tubes in compression. In Proceedings of the 2015 World Congress on Advances in Structural Engineering and Mechanics (ASEM15), Incheon, Korea, 25–29 August 2015; pp. 1–15.

4. Fakharifar, M.; Chen, G. Compressive behavior of FRP-confined concrete-filled PVC tubular columns. *Compos. Struct.* **2016**, *141*, 91–109. [[CrossRef](#)]
5. Oyawa, W.O.; Gathimba, N.K.; Mang'uriu, G.N. Structural response of composite concrete filled plastic tubes in compression. *Steel Compos. Struct.* **2016**, *21*, 589–604. [[CrossRef](#)]
6. Gathimba, N.K.; Oyawa, W.O.; Mang'uriu, G.N. Performance of UPVC Pipe Confined Concrete Columns in Compression. MSc. Thesis, Jomo Kenyatta University of Agriculture and Technology, Juja, Kenya, 2015.
7. Gupta, P.K. Confinement of concrete columns with unplasticized Poly-vinyl chloride tubes. *Int. J. Adv. Struct. Eng.* **2013**, *5*, 1–8. [[CrossRef](#)]
8. Gupta, P.K.; Verma, V.K. Study of concrete-filled unplasticized poly-vinyl chloride tubes in marine environment. *Proc. Inst. Mech. Eng. Part M J. Eng. Marit. Environ.* **2014**, *230*, 229–240. [[CrossRef](#)]
9. Fakharifar, M.; Chen, G. FRP-confined concrete filled PVC tubes: A new design concept for ductile column construction in seismic regions. *Constr. Build. Mater.* **2017**, *130*, 1–10. [[CrossRef](#)]
10. Ranney, T.; Parker, L. *Susceptibility of ABS, FEP, FRE, FRP, PTFE, and PVC Well Casing to Degradation by Chemicals*; US Army Corps of Engineers (Report No. 195-1); USACE: Washington, DC, USA, 1995. Available online: <https://usace.contentdm.oclc.org/digital/collection/p266001coll1/id/6165/> (accessed on 5 December 2018).
11. Folkman, S. Validation of the long life of PVC pipes. In Proceedings of the 17th Plastic Pipes Conference, Chicago, IL, USA, 22–24 September 2014; pp. 1–9.
12. Boersma, A.; Breen, J. Long term performance prediction of existing PVC water distribution systems. In Proceedings of the 9th International Conference PVC, Brighton, UK, 26–28 April 2005.
13. Breen, J. *Expected Lifetime of Existing Water Distribution Systems-Management Summary*; TNO: The Hague, The Netherlands, 2006.
14. Burn, S.; Davis, P.; Schiller, T. *Long-Term Performance Prediction for PVC Pipes*; Water Research Foundation: Denver, CO, USA, 2006.
15. Wang, J.Y.; Yang, Q.B. Investigation on compressive behaviors of thermoplastic pipe confined concrete. *Constr. Build. Mater.* **2012**, *35*, 578–585. [[CrossRef](#)]
16. Wang, J.; Yang, Q. Experimental Study on Mechanical Properties of Concrete Confined with Plastic Pipe. *ACI Mater. J.* **2010**, *107*, 132–137.
17. Xue, J.; Li, H.; Zhai, L.; Ke, X.; Zheng, W.; Men, B. Analysis of mechanical behavior and influencing factors of high strength concrete columns with PVC pipe under repeated loading. *J. Xi'an Univ. Archit. Technol.* **2016**, *48*, 24–28.
18. Wang, K.; Young, B. Fire resistance of concrete-filled high strength steel tubular columns. *Thin-Walled Struct.* **2013**, *71*, 46–56. [[CrossRef](#)]
19. Jamaluddin, N.; Azeez, A.A.; Rahman, N.A.; Attiyah, A.N.; Ibrahim, M.W.; Mohamad, N.; Adnan, S.H. Experimental Investigation of Concrete Filled PVC Tube Columns Confined by Plain PVC Socket. In Proceedings of the MATEC Web Conference, Wuhan, China, 20–21 December 2017.
20. Marzoucka, M.; Sennah, K. Concrete filled PVC tubes as compression members. In Proceedings of the International Seminar, Composite Material in Concrete Construction, Dundee, Scotland, UK, 5–6 September 2002; pp. 31–38.
21. Saadoun, A.S. Experimental and Theoretical Investigation of PVC-Concrete Composite Columns. Ph.D. Thesis, University of Basrah, Basra, Iraq, 2010.
22. Kurt, C.E. Concrete Filled Structural Plastic Columns. *J. Struct. Div.* **1978**, *104*, 55–63.
23. British Standard Institution. *BS EN 932-1 Tests for General Properties of Aggregates: Part 1. Methods for Sampling*; British Standard Institution: London, UK, 1997.
24. British Standard Institution. *BS EN 933-1 Tests for Geometrical Properties of Aggregates Part 1: Determination of Particle Size Distribution—Sieving Method*; British Standard Institution: London, UK, 2012.
25. BSI Standards Ltd. *BS EN 933-2 Tests for Geometrical Properties of Aggregates. Determination of Particle Size Distribution. Test Sieves, Nominal Size of Apertures*; BSI Standards Ltd.: London, UK, 1996.
26. BSI Standards Ltd. *BS EN 1097-6 Tests for Mechanical and Physical Properties of Aggregates Part 6: Determination of Particle Density and Water Absorption*; BSI Standards Ltd.: Brussels, Belgium, 2013.
27. BSI Standards Ltd. *BS EN 1097-5 Tests for Mechanical and Physical Properties of Aggregates Part 5. Determination of the Water Content by Drying in a Ventilated Oven*; British Standards Institution (BSI): London, UK, 2008.
28. European Standard. *EN 197-1 Cement. Composition, Specifications and Conformity Criteria for Common Cements*; European Standard: Brussels, Belgium, 2011.

29. BSI Standards Ltd. *BSI BS EN 206:2013: Concrete. Specification, Performance, Production and Conformity*; BSI Standards Ltd.: London, UK, 2013.
30. BSI Standards Ltd. *BSI BS 8500-1:2006 + A1:2012 Concrete. Complementary British Standard to BS EN 206-1. Method of Specifying and Guidance for the Specifier*; BSI Standards Ltd.: London, UK, 2012.
31. BSI Standards Ltd. *BS EN 12350-1 Testing Fresh Concrete, Part 1: Sampling Fresh Concrete*; BSI Standards Ltd.: London, UK, 2009.
32. BSI Standards Ltd. *BS EN 12350-2 Testing Fresh Concrete, Part 2: Slump Test*; BSI Standards Ltd.: London, UK, 2009.
33. BSI Standards Ltd. *BS EN 12350-6 Testing Fresh Concrete, Part 6: Fresh Density*; BSI Standards Ltd.: London, UK, 2009.
34. BSI Standards Ltd. *BS 1881-103 Testing Concrete, Part 103: Method for Determination of Compacting Factor*; BSI Standards Ltd.: London, UK, 1993.
35. ASTM International. *ASTM D638 Standard Test Method for Tensile Properties of Plastics*; ASTM: West Conshohocken, PA, USA, 2014; ISBN 0521298466.
36. Fakharifar, M.; Dalvand, A.; Sharbatdar, M.K.; Chen, G.; Sneed, L. Innovative hybrid reinforcement constituting conventional longitudinal steel and FRP stirrups for improved seismic strength and ductility of RC structures. *Front. Struct. Civ. Eng.* **2016**, *10*, 44–62. [[CrossRef](#)]
37. Chen, Y.; Feng, R.; Xiong, L. Experimental and numerical investigations on steel-concrete-PVC SHS joints under axial compression. *Constr. Build. Mater.* **2016**, *102*, 654–670. [[CrossRef](#)]
38. BSI. *BSI Testing Hardened Concrete. Making and Curing Specimens for Strength Tests*; BSI: London, UK, 2009; ISBN 0 580 36604 9.
39. ASTM. *ASTM C39/C39M-12, Standard Test Method for Compressive Strength of Cylindrical Concrete Specimens*; ASTM: West Conshohocken, PA, USA, 2012; ISBN 5919881100.
40. Cui, C.; Sheikh, S.A. Experimental Study of Normal- and High-Strength Concrete Confined with Fiber-Reinforced Polymers. *J. Compos. Constr.* **2010**, *14*, 553–561. [[CrossRef](#)]
41. Najdanović, D.; Milosavljević, B. Strength and ductility of concrete confined circular columns. *J. Croat. Assoc. Civ. Eng.* **2014**, *66*, 417–423.
42. Zhang, X.-H.; Lu, X.-B.; Zhang, L.-M.; Wang, S.-Y.; Li, Q.-P. Experimental study on mechanical properties of methane-hydrate-bearing sediments. *Acta Mech. Sin.* **2012**, *28*, 1356–1366. [[CrossRef](#)]
43. Wu, Y.F. The effect of longitudinal reinforcement on the cyclic shear behavior of glass fiber reinforced gypsum wall panels: Tests. *Eng. Struct.* **2004**, *26*, 1633–1646. [[CrossRef](#)]
44. Karabinis, A.I.; Rousakis, T.C. Concrete confined by FRP material: A plasticity approach. *Eng. Struct.* **2002**, *24*, 923–932. [[CrossRef](#)]
45. Richart, F.; Brandtzaeg, A.; Brown, R.L. *A Study of the Failure of Concrete under Combined Compressive Stresses*; University of Illinois at Urbana Champaign, College of Engineering. Engineering Experiment Station: Champaign, IL, USA, 1928; Volume 26.
46. Saatcioglu, B.M.; Razvi, S.R. Strength and ductility of confined concrete. *J. Struct. Eng.* **1992**, *118*, 1590–1607. [[CrossRef](#)]
47. Bisby, L.A.; Dent, A.J.S.; Green, M.F. Comparison of Confinement Models for Fiber-Reinforced Polymer-Wrapped Concrete. *ACI Struct. J.* **2005**, *102*, 62–72.
48. Cusson, D.; Paultre, P. Stress-Strain Model for Confined High-Strength Concrete. *J. Struct. Eng.* **1995**, *121*, 468–477. [[CrossRef](#)]
49. Benzaid, R.; Mesbah, H.; Chikh, N.E. FRP-confined concrete cylinders: Axial compression experiments and strength model. *J. Reinf. Plast. Compos.* **2010**, *29*, 2469–2488. [[CrossRef](#)]
50. Xiao, Q.G.; Teng, J.G.; Yu, T. Behavior and Modeling of Confined High-Strength Concrete. *J. Compos. Constr.* **2010**, *14*, 249–259. [[CrossRef](#)]

